Catalysis Letters, Vol. 116, Nos. 1–2, July 2007 (© 2007)
DOI: 10.1007/s10562-007-9085-x

Catalytic activities and properties of mesoporous sulfated Al_2O_3–ZrO_2

Jie Zhao, Yinghong Yue, Weiming Hua,* and Zi Gao

Department of Chemistry and Shanghai Key Laboratory of Molecular Catalysis and Innovative Materials, Fudan University, Shanghai 200433, P.R. China

Received 9 March 2007; accepted 9 March 2007

Mesoporous sulfated Al_2O_3–ZrO_2 (MSAZ) catalysts with large surface areas and pore volumes after calcination at high temperature (650 °C) and with higher Al_2O_3 content than 20wt% were successfully prepared from a template of block copolymer (P84). The MSAZ catalysts were characterized by X-ray diffraction (XRD), N_2 adsorption, transmission electron microscopy (TEM), ^{27}Al magic-angle spinning nuclear magnetic resonance (MAS NMR), thermogravimetric analysis (TG–DTG), temperature-programmed desorption of ammonia (NH_3-TPD) and infrared spectra (IR) of adsorbed pyridine. It is shown that the resulting mesostructured sulfated Al_2O_3–ZrO_2 samples have a well-developed textural mesoporosity. The number of acid sites present on MSAZ catalysts is higher than that on conventional sulfated zirconia, and the former catalysts are more active than the latter one for various acid-catalyzed reactions.

KEY WORDS: mesostructured; sulfated alumina-zirconia; tetragonal crystalline; acid-catalyzed reactions.

1. Introduction

Conventional industrial acid catalysts, such as sulfuric acid, $AlCl_3$ and BF_3, have unavoidable drawbacks, because they are corrosive, environmentally unfriendly, uneasy to separate from liquid products and susceptible to water. The search for economical and ecological solid acids has driven the worldwide ongoing research of new materials replacing current liquid acids and halogen-based solid acids [1]. Among them sulfated zirconia (SZ), as an environmentally benign solid superacid, has attracted intense attention in the last 20 years, because this catalyst is highly acidic and has potential application in acid-catalyzed reactions of industrial importance, such as hydrocarbon isomerization, alkylation, acylation, esterification and etc. [2–4]. To generate strong acidity, sulfated zirconia must be calcined in air at high temperatures. Calcination temperature plays a crucial role in its acidity and catalytic properties. To make SZ catalyst extremely acidic and highly active for hydrocarbon isomerization, the optimal calcination temperature was 600–650 °C [5–9]. After calcination at such high temperature, the specific surface area of the resulting material is usually at around 80–100 m^2/g. The relatively small surface area and non-uniform pore size limits its potential applications.

High surface area is available by supporting SZ into the pores of mesoporous silica [10–16], such as MCM-41, SBA-15 and HMS, but the resulting materials show low catalytic activity for alkane isomerization [10,11], if the activity is expressed as conversion under the same catalyst weight. The possible reason is due to a decrease in acid strength. Several successful examples of preparing mesoporous SZ with high surface area have been reported [17–20]. However, most synthetic routes typically yielded products with amorphous framework walls, which brought about relatively low activity for alkane isomerization compared with conventional sulfated zirconia catalyst. Moreover, the thermal stability of mesostructure is relatively poor, and these materials would lose their mesostructure after calcination over 550 °C.

Our earlier studies showed that incorporating small amounts of Al_2O_3 into SZ enhanced substantially the catalytic activity and also improved resistance to deactivation at high temperature (250 °C) for *n*-butane isomerization in the presence of H_2 [21–23]. This remarkable promoting effect was most likely attributed to due to a different distribution of acid sites strength and to an enhanced number of acid sites with intermediate strength. Since then, several groups have contributed to Al-promoted sulfated zirconia (SAZ) [24–29]. However, when the Al_2O_3 content exceeds 10wt%, the activity of SAZ catalyst is very low, obviously lower than that of SZ [21,25]. The reason is due to the absence of crystalline zirconia phases.

The purpose of this work is to prepare mesoporous sulfated Al_2O_3–ZrO_2 (MSAZ) catalysts with large surface areas after calcination at high temperature (650 °C) and with higher Al_2O_3 content than 20wt% by liquid-crystal templating method. Furthermore, catalytic tests in conversion of *n*-pentane, Friedel–Crafts benzoylation of toluene with benzoyl chloride and dealkylation of 1,3,5-tri-tert-butyl-benzene show that MSAZ catalysts

*To whom correspondence should be addressed.
E-mail: wmhua@fudan.edu.cn

are more active than conventional sulfated zirconia at appropriate content of alumina. The textural properties as well as acidic properties of the catalysts were characterized.

2. Experimental

2.1. Preparation of catalysts

Mesoporous alumina–zirconia mixed oxides were prepared according to the method reported by Zhang and co-workers [30]. An aqueous solution containing suitable amounts of $Al(NO_3)_3$ and $ZrOCl_2$ was mixed with desired amount of the tri-block $(EO)_{19}(PO)_{39}(EO)_{19}$ surfactant Pluronic P84 ((Al + Zr): P84 = 1:0.015 molar ratio). The resulting mixture was aged under stirring at 45 °C for 36 h, and then at 90°C for additional 6 h. Aqueous ammonia was slowly added under gentle stirring until the final pH was near 8. The solid gel was aged at room temperature for 6 h, and then put into an autoclave. After sealed, the autoclave was maintained at 100 °C for 24 h. The product was filtered, washed, dried, calcined at 325 °C for 3 h and then at 500 °C for 4 h in flowing air to remove the surfactant. Mesoporous sulfated alumina-zirconia were prepared by immersing mesostructured Al_2O_3–ZrO_2 mixed oxides in a 0.5 M H_2SO_4 solution for 1 h, followed by filtering, drying and calcination at 650 °C in static air for 3 h. The obtained catalysts are labeled as x%MSAZ, where x% represents the weight percentage of zirconia in the catalysts. Conventional sulfated zirconia (denoted as CSZ) was made by immersing dried $Zr(OH)_4$ in a 0.5 M H_2SO_4 solution, followed by calcination at 650 °C in static air for 3 h. HY zeolite with a Si/Al of 2.6 was prepared from NaY by ion exchange with NH_4Cl solution and calcined at 350 °C.

2.2. Characterization of catalysts

X-ray powder diffraction patterns were recorded on a Rigaku D/MAX-IIA diffractometer using Cu Kα radiation (λ = 1.5405 Å) at 30 kV and 20 mA. The crystallite size of tetragonal ZrO_2 phase was determined from the characteristic peak (2θ = 30.18° for the (111) reflection) using Scherrer equation: $D = K_{\overline{W}}\cos\theta$, where K = 0.9, D represents crystalline size, λ represents the wavelength of Cu Kα radiation, and $W = W_b - W_s$; W_b is the broadened profile width of experimental sample and W_s is the standard profile width of reference silica sample. The N_2 adsorption–desorption isotherms were measured on a Micromeritics ASAP2000 instrument at liquid N_2 temperature. Pore size distributions were calculated from the adsorption isotherms by the Barrett–Joyner–Halenda (BJH) model. Specific surface areas of the catalysts were calculated from the adsorption isotherms by the Brunauer–Emmett–Teller (BET) method. Transmission electron microscopy and electron diffraction patterns of selected areas were obtained on a JEOL-2010 instrument. ^{27}Al magic-angle spinning nuclear magnetic resonance spectra were recorded on a Bruker DSX-300 spectrometer. A resonance frequency of 78.2 MHz, a recycle delay of 0.2 s, short 0.3 μs pulses, a spectral width of 59 kHz and a spin rate of 12 kHz were applied. Thermogravimetric measurements were carried out on a Rigaku thermoflex instrument in flowing air from room temperature to 1100 °C at a heating rate of 10 °C/min. The temperature-programmed desorption of ammonia was performed in a flow-type fixed-bed reactor at ambient pressure. The catalyst was pretreated at 600 °C for 2 h and then cooled to 120 °C in He flow. Pure NH_3 was injected until adsorption saturation, followed by purging with He for 2 h. The temperature was then raised from 120 to 670 °C at a rate of 10 °C/min. The NH_3 desorbed was collected in a liquid N_2 trap and analyzed by gas chromatography. Infrared (IR) spectra of pyridine adsorption were recorded on a Nicolet Nexus 470 FT-IR spectrometer which was furnished with an in situ sample cell. A self-supporting disk of the sample (14.4 mg) was pretreated at 300°C for 4 h under a vacuum of 10^{-2} Pa and then cooled to 150 °C. After the pyridine adsorption at 150 °C for 30 min and evacuation at a desired temperature for 30 min, IR spectra were recorded.

2.3. Activity tests

The conversion of *n*-pentane was performed at 30 °C in a closed reaction system. After catalyst (0.5 g) was placed in the reactor and pretreated in a vacuum at 350 °C for 3 h, 25 μL of *n*-pentane was introduced into the reaction system. After reaction for 2.5 h, the products were analyzed by a gas chromatograph equipped with a flame ionization detector (FID). Benzoylation of toluene was carried out at 110 °C in a three necked round bottom flask fitted with a magnetic stirrer, a thermometer and a reflux condenser with NaOH-tube. A mixture of 10 mL of toluene, 1.7 mmol of benzoyl chloride and 400 mg of catalyst was added to the flask. After reaction for 5 h, the products were analyzed by a gas chromatograph equipped with FID. The dealkylation of 1,3,5-tri-tert-butyl-benzene (TTBB) was performed in a pulsed microreactor. The catalyst load was 10 mg, and the catalyst was preheated at 450 °C in argon for 2 h before reaction. Argon with a flow rate of 60 mL/min was used as the carrier gas. The reaction temperature was 200 °C, and 5 μL of a mixture of TTBB and cyclohexane (1:3 molar ratio) was injected for each test. The products were analyzed by a gas chromatograph equipped with a thermal conductivity detector (TCD).

3. Results and discussion

3.1. Catalyst characterization

XRD patterns of MSAZ and CSZ catalysts calcined at 650 °C for 3 h are shown in figure 1. The peaks at 30.2, 35.3, 50.4 and 59.7° are the diffractions of (111), (200), (220) and (131) of tetragonal ZrO_2, respectively, whereas the peak at 28.2° is the diffraction of $(11\bar{1})$ of monoclinic ZrO_2. The peaks at 66.8 and 45.8° are assigned to the diffractions of (440) and (400) of γ-Al_2O_3, respectively. It can be seen that a small portion of monoclinic ZrO_2 phase is presented in CSZ along with the tetragonal ZrO_2 phase. For MSAZ catalysts only the tetragonal phase exists, indicating that the transformation of ZrO_2 from the metastable tetragonal phase to the monoclinic phase is retarded in the presence of alumina. Similar phenomenon was observed in our previous work [21,23]. As the ZrO_2 content is increased, the intensity of characteristic diffractive peaks of the tetragonal phase increases progressively, whereas that of the γ-Al_2O_3 phase decreases gradually. The diffractive peaks of γ-Al_2O_3 are not observed in MSAZ catalysts containing 60wt% or more ZrO_2. The peak narrowing with increasing ZrO_2 content is attributed to the large crystallite size of zirconia. The peak broadening of ZrO_2 in MSAZ catalysts in comparison with CSZ suggests that the former catalysts have smaller crystallite size of zirconia, as shown in table 1. This result demonstrates that the growth of zirconia crystallite size is inhibited in the presence of alumina.

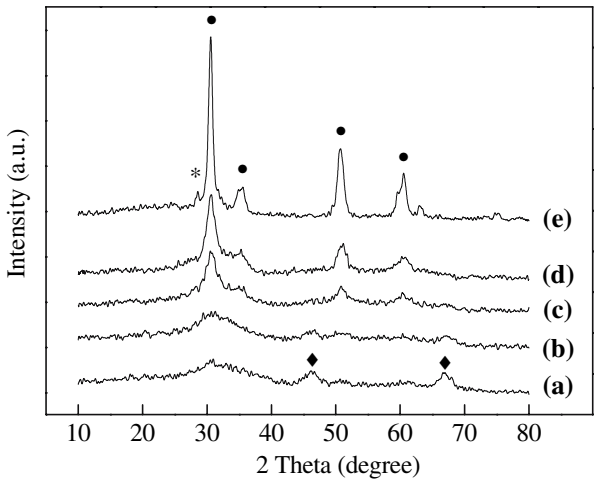

Figure 1. XRD patterns of the catalysts calcined at 650 °C. (a) 20%MSAZ, (b) 40%MSAZ, (c) 60%MSAZ, (d) 80%MSAZ, (e) CSZ. (*) Monoclinic ZrO_2, (●) tetragonal ZrO_2, (◆) γ–Al_2O_3.

Zirconia may exist in two crystalline phases after calcination below 800 °C: a metastable tetragonal phase and a thermodynamically favored monoclinic phase [31]. It is generally believed that the presence of a stable tetragonal ZrO_2 phase is a necessary condition for the formation of superacidity in sulfated zirconia and its analogues, and good catalytic activity is considered to be connected to tetragonal zirconia [7,19,32–34]. Attempts have been made to synthesize catalytically active monoclinic sulfated zirconia. However, the resulting materials exhibit lower activity in *n*-butane isomerization than tetragonal sulfated zirconia [35–37]. In our case, ZrO_2 in MSAZ catalysts exists in a pure tetragonal phase, suggesting the possibility for the formation of superacidity.

Figure 2 illustrates the N_2 adsorption–desorption isotherms of MSAZ catalysts calcined at 650 °C for 3 h. They display characteristic type IV adsorption isotherm, which is generally observed for mesoporous materials. Hysteresis between the adsorption and desorption branches observed for the MSAZ catalysts is of type H2 based on international union of pure and applied chemistry (IUPAC) classifications. A sharp inflection in the N_2 adsorption isotherm at around $P/P_0 = 0.4$ shows the capillary condensation within the mesopores after the formation of monolayer. The BJH pore size distributions of MSAZ catalysts, calculated from the adsorption data, are shown in figure 3. The pore diameters are narrow in distribution, and the pore size at the maximum of the distribution is progressively shifted from 4.93 to 3.33 nm with an increment of ZrO_2 content (also see table 1). The above results indicate that the mesoporosity is well preserved after heating the catalysts at 650 °C, suggesting the high thermal stability of mesostructure for mesoporous sulfated Al_2O_3–ZrO_2 as-prepared in the present work.

The BET specific surface area, pore volume and the most probable pore diameter of the catalysts are summarized in table 1. As the ZrO_2 content is increased, the surface area and pore volume of MSAZ catalysts decline gradually, ranging from 262 to 165 m^2/g and from 0.340 to 0.156 mL/g, respectively. Obviously, the MSAZ catalysts have much larger surface area and pore volume

Table 1
Textural properties of the catalysts

Catalyst	BET(m^2/g)	Pore volume (mL/g)	Pore size (nm)	Sulfate content (wt%)	Crystallite size (nm)
20%MSAZ	262	0.340	4.93	7.7	1.7
40%MSAZ	226	0.283	4.45	8.4	1.9
60%MSAZ	193	0.237	4.33	8.4	3.4
80%MSAZ	165	0.156	3.33	7.0	4.9
CSZ	82	0.087	–	3.1	14.2

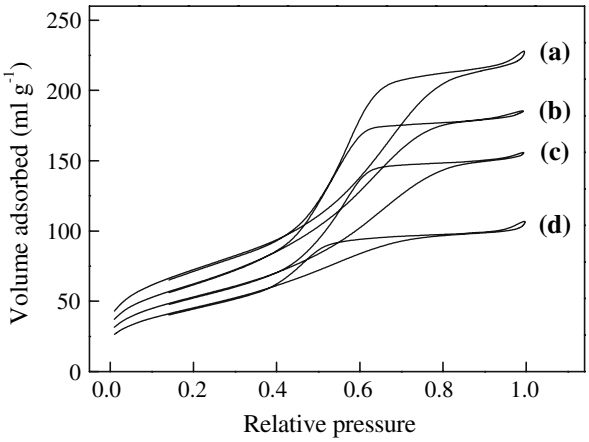

Figure 2. N_2 adsorption–desorption isotherms of the catalysts. (a) 20%MSAZ, (b) 40%MSAZ, (c) 60%MSAZ, (d) 80%MSAZ.

than conventional sulfated zirconia, implying that the former catalysts would exhibit higher catalytic activities since heterogeneously catalyzed reactions occur at the solid/fluid interface. Based on the t-plot analysis, the contribution from micropores to the measured surface area and pore volume is negligible for the MSAZ catalysts. It is therefore clear that a series of mesoporous sulfated Al_2O_3–ZrO_2 materials with large surface areas and pore volumes after calcination at high temperature (650 °C) are successfully obtained.

The TEM image of 60%MSAZ is given in figure 4. The regular worm-like channels with no discernible long-range packing order are observed. The selected-area electron diffraction patterns recorded for the catalyst display clear diffuse electron diffraction rings, suggesting that the channel walls are composed of small crystallites. This result is consistent with the XRD observation.

To investigate the coordination environment of aluminum in MSAZ catalysts, ^{27}Al MAS NMR spectroscopic measurement was performed on a Bruker DSX-300 spectrometer. Figure 5 shows ^{27}Al MAS NMR spectra of 20%MSAZ, 40%MSAZ and 60%MSAZ. All the catalysts display two resonance signals. The intense peak at around 2 ppm is assigned to six-coordinate aluminum, while the weak peak centered at around 60 ppm is ascribed to four-coordinate aluminum. It is clear that the six-coordinate aluminum species is dominant in the catalysts. The ratio of four- and six-coordinate aluminum is ca. 1:3, as expected for the γ-phase alumina [38]. This signifies the presence of γ-phase alumina in the channel walls of the catalysts, which is in agreeable with the XRD result. Unobservable five-coordinate aluminum resonance near 35 ppm suggests the absence of appreciable quantities of amorphous alumina domains in the mesostructued channel walls.

The TG–DTG profile of 60%MSAZ as a representative sample is depicted in figure 6. The TG curve presents two weight losses at 15–280 °C and

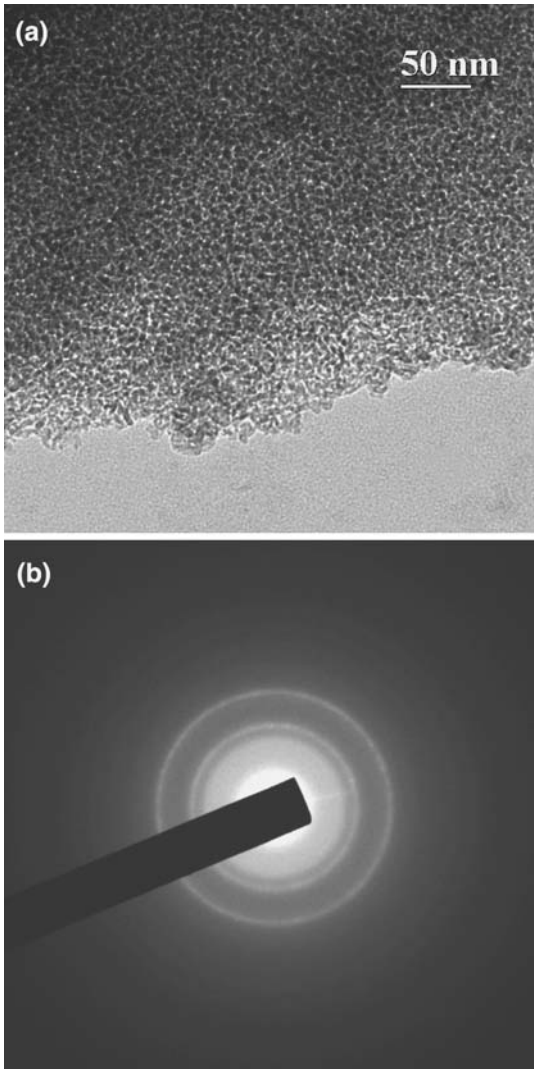

Figure 4. TEM image (a) and selected-area electron diffraction patterns (b) of the 60%MSAZ catalyst.

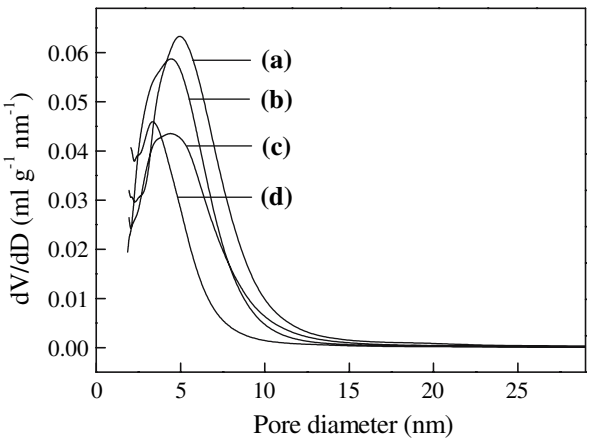

Figure 3. Pore size distributions of the catalysts. (a) 20%MSAZ, (b) 40%MSAZ, (c) 60%MSAZ, (d) 80%MSAZ

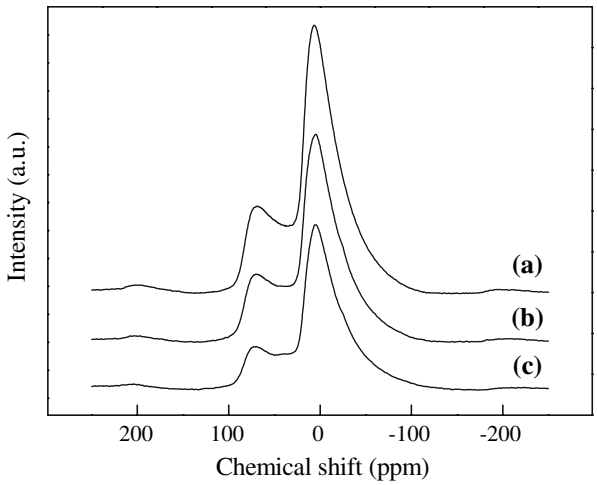

Figure 5. ^{27}Al MAS NMR spectra of the catalysts. (a) 20%MSAZ, (b) 40%MSAZ, (c) 60%MSAZ.

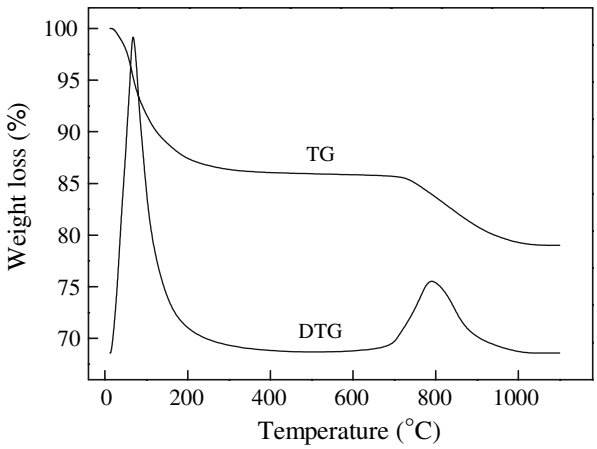

Figure 6. TG–DTG curves of the 60%MSAZ catalyst

700–1050 °C over the whole range of studied temperature. Accordingly, two weight loss peaks are observed on the DTG curve. The quick weight loss peak at 67 °C corresponds to the desorption of adsorbed water, while the high-temperature weight loss peak is assigned to the decomposition of sulfate species in the catalyst. Based on the amount of weight loss, the sulfate content contained in the catalysts has been calculated and listed in table 1. The sulfate content of MSAZ catalysts is 7.0–8.4wt%, which is much higher than that of CSZ. An abundance of surface sulfate species may imply that MSAZ catalysts contain greater number of strong acidic and superacidic sites.

The surface acidity of the catalysts was measured by NH_3-TPD method. The NH_3-TPD profiles of MSAZ and CSZ catalysts after calcination at 650 °C are shown in figure 7. The CSZ catalyst presents only one broad peak of desorption at about 245 °C. Different from CSZ, the MSAZ catalysts exhibit two desorption peaks. The low temperature peak is centered at around 240 °C,

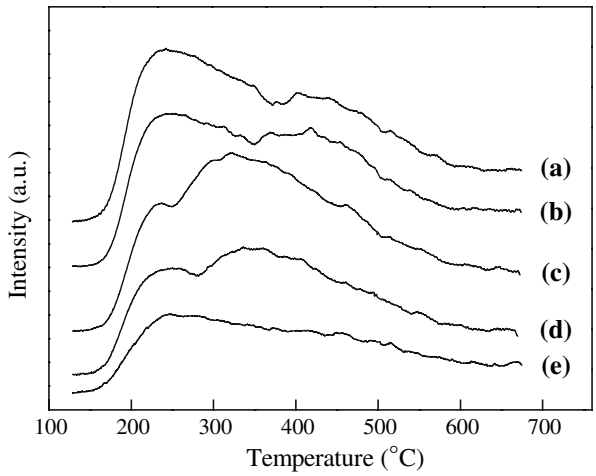

Figure 7. NH_3-TPD profiles of the catalysts. (a) 20%MSAZ, (b) 40%MSAZ, (c) 60%MSAZ, (d) 80%MSAZ, (e) CSZ

and the high temperature peak is in the range of 320–420 °C. Moreover, the peak areas of MSAZ catalysts are larger than that of CSZ, suggesting that the former catalysts have higher concentrations of acid sites. The NH_3-TPD data are listed in table 2. NH_3 molecules desorbing between 120 and 500 °C correspond to acidity with weak and medium acid strength, and those desorbing between 500 and 670 °C correspond to acidity with strong and very strong acid strength (or superacid strength) [39,40]. As the ZrO_2 content is increased, the number of total acid sites as well as weak and medium strong acid sites presented on the MSAZ catalysts declines gradually, while that of strong and very strong acid sites increases progressively. This can be understandable since strong acidity and superacidity are originated from sulfated zirconia. It is clear that the acidity of MSAZ catalysts is obviously higher than that of CSZ.

The type of acid sites (Lewis and Brønsted) was measured *in situ* by pyridine adsorption spectra. Figure 8 shows the IR spectra of the 60%MSAZ catalyst after adsorption of pyridine and desorption at 150 and 300 °C. Both Lewis (at 1450 cm^{-1}) and Brønsted (1540 cm^{-1}) acid sites are present on the catalyst. When the pyridine desorption temperature increased from 150 to 300° C, the intensity of the peak at 1450 cm^{-1}

Table 2
NH_3-TPD data of the catalysts

Catalyst	NH_3 desorbed (mmol/g)		
	120–500 °C	500–670 °C	Total
20%MSAZ	0.75	0.16	0.91
40%MSAZ	0.73	0.16	0.89
60%MSAZ	0.68	0.18	0.86
80%MSAZ	0.61	0.19	0.80
CSZ	0.43	0.14	0.57

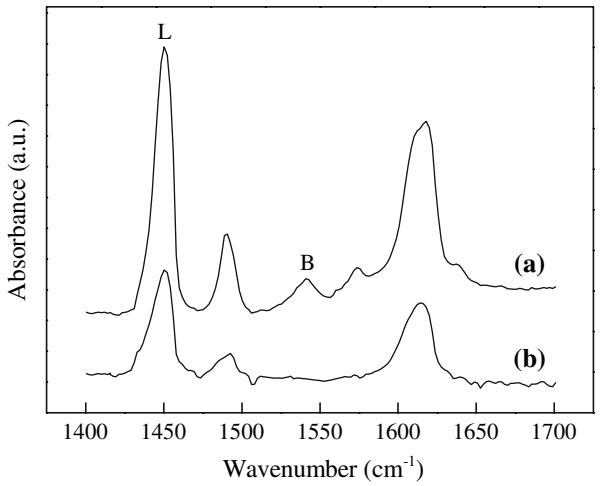

Figure 8. *In situ* IR spectra of the 60%MSAZ catalyst after adsorption of pyridine and desorption at (a) 150 °C and (b) 300 °C.

decreases, while that at 1540 cm^{-1} disappears, suggesting that the strength of Lewis acid sites is stronger than that of Brønsted ones.

3.2. Catalytic testing

At ambient temperature the conversion of *n*-pentane proceeds only on solid acids with strong acidity or superacidity, such as SO_4^{2-}/ZrO_2, SO_4^{2-}/TiO_2, SO_4^{2-}/Fe_2O_3 and HM zeolite [41]. The activities of MSAZ and CSZ catalysts for *n*-pentane conversion at 30 °C are given in table 3. The major reaction products are isopentane and isobutane. At high conversion level, very small amounts of C_3, *n*-C_4 and C_6 hydrocarbons are detected. The conversion of *n*-pentane on MSAZ catalysts increases with increasing the ZrO_2 content, and both 60%MSAZ and 80%MSAZ catalysts have higher conversion than CSZ. This can be probably attributed to greater number of very strong acid sites possessed by the former two catalysts. Previous work on Al-promoted SZ (SAZ) showed that SAZ catalyst with higher alumina content than 10wt% displayed substantially lower activity for small alkane conversion (e.g. *n*-butane isomerization) than conventional sulfated zirconia, which is due to the fact that zirconia in SAZ catalyst is amorphous [21,25]. Our present work shows that zirconia in MSAZ catalysts with higher alumina content than 20wt% is tetragonal phase, which is known to be necessary for the generation of superacidity in sulfated zirconia [7,19,32–34]. This is the reason for the difference on activity for small alkane conversion between this work and literature [21,25].

Table 3
Reaction data for the conversion of *n*-pentane at 30 °C

Catalyst	Conversion (%)	Product distribution (mol%)	
		i-C_4	i-C_5
20%MSAZ	4.8	0	100
40%MSAZ	16.3	36.4	63.6
60%MSAZ	49.1	85.7	14.3
80%MSAZ	54.3	79.5	20.5
CSZ	40.7	87.8	12.2

Table 4
Reaction data for benzoylation of toluene with benzoyl chloride at 110 °C

Catalyst	Conversion (%)	Product distribution (mol%) [a]		
		o-MBP	m-MBP	p-MBP
20%MSAZ	5.4	28.0	3.9	68.1
40%MSAZ	12.5	28.0	3.0	69.0
60%MSAZ	30.5	26.9	4.1	69.0
80%MSAZ	39.0	27.3	3.8	68.9
CSZ	25.9	27.7	2.7	69.6

[a] MBP = methylbenzophenone.

Friedel–Crafts acylation of aromatics is an important reaction producing valuable chemical intermediates. Benzoylation of toluene with benzoyl chloride was used as a test reaction to investigate the activities of MSAZ and CSZ catalysts for this type of liquid-phase acid-catalyzed reactions. As shown in table 4, the reaction products are a mixture of p-, o- and m-methylbenzophenone, and the proportions of the isomers are in the range of p-methylbenzophenone 68–70%, o-methylbenzophenone 27–28% and m-methylbenzophenone 3–4%. The conversion of benzoyl chloride on MSAZ catalysts increases with increasing the ZrO_2 content. Both 60%MSAZ and 80%MSAZ catalysts have higher conversion than CSZ, which is due to the fact that the former catalysts have greater number of strong and very strong acid sites, as revealed by NH_3-TPD result (see table 2). Under the same reaction conditions, the HY zeolite is inactive for this reaction. The reason is the lack of very strong acid sites or superacidity for HY [42]. These results suggest that mesoporous MSAZ are superior candidates as catalysts for strong and very strong acid-catalyzed reactions.

Table 5
Reaction data for 1,3,5-tri-tert-butyl-benzene dealkylation at 200 °C

Catalyst	Conversion (%)	Product distribution (mol%) [a]	
		TBB	DTBB
20%MSAZ	81.2	20.4	79.6
40%MSAZ	81.9	30.9	69.1
60%MSAZ	88.1	38.2	61.8
80%MSAZ	80.7	35.2	64.8
CSZ	68.7	24.3	75.7
HY	6.7	–	100

[a] TBB = tert-butyl-benzene, DTBB = di-tert-butyl-benzene.

The dealkylation of 1,3,5-tri-tert-butylbenzene with a molecular dimension of 0.94 nm was chosen as a model acid-catalyzed reaction of large molecules. The reaction data are listed in table 5. The selectivity to di-tert-butylbenzene is much higher than that to tert-butyl-benzene. The conversion of MSAZ catalysts is 81–88%, obviously higher than that of CSZ. This can be attributed to higher concentrations of acid sites presented on the former catalysts, as revealed by NH_3-TPD result (see table 2). Under the same reaction conditions, the conversion of HY zeolite is only 6.7, albeit it has 3.45 mmol g^{-1} acid sites [43]. This is due to the fact that the pore size of HY is small and the catalytic reaction can only occur on the external surface of HY crystals. These results elucidate the advantages of using mesoporous MSAZ as catalysts for catalytic reactions of bulky molecules, such as those encountered in the production of pharmaceuticals and fine chemicals. Although zeolites are widely used in acid-catalyzed industrial processes, their small pore size makes them relatively poor catalysts in the case of catalytic reactions of bulky molecules due to slow diffusion of reactants through the zeolitic microporous structure.

4. Conclusions

In the present work we have shown that mesostructured sulfated Al_2O_3–ZrO_2 (MSAZ) catalysts with large surface areas and pore volumes after calcination at high temperature and with higher alumina content than 20wt% were successfully synthesized. Zirconia in MSAZ catalysts is tetragonal crystalline. MSAZ catalysts have much higher surface area, pore volume and sulfate content than conventional sulfated zirconia (CSZ). The nature of acid sites present on the catalysts is Lewis and Brønsted type, and the strength of Lewis acid sites is stronger than that of Brønsted ones. MSAZ catalysts have greater number of strong and very strong acid sites than CSZ. Catalytic tests show that mesoporous sulfated Al_2O_3–ZrO_2 catalysts exhibit higher activities than conventional sulfated zirconia for conversion of n-pentane, Friedel–Crafts benzoylation of toluene with benzoyl chloride and dealkylation of 1,3,5-tri-tert-butyl-benzene. Catalytic evaluation for the dealkylation of 1,3,5-tri-tert-butylbenzene shows that mesostructured MSAZ catalysts provide potential application for catalyzing bulky molecules and elucidate the advantages over microporous zeolites.

Acknowledgments

This work was financially supported by the State Basic Research Project of China (2006CB806103), the National Natural Science Foundation of China (20633030 and 20303004).

References

[1] K. Tanabe, M. Misono, Y. Ono and H. Hattori, *New Solid Acids and Bases* (Kodansha, Tokyo, 1989).
[2] A. Corma, Chem. Rev. 95 (1995) 559.
[3] X. Song and A. Sayari, Catal. Rev. Sci. Eng. 38 (1996) 329.
[4] G.D. Yadav and J.J. Nair, Micropor. Mesopor. Mater. 33 (1999) 1.
[5] M. Hino and K. Arata, J. Chem. Soc. Chem. Commun. (1980) 851.
[6] Z. Gao, J.M. Chen and Y. Tang, Chem. J. Chin. Univ. 12 (1992) 1498.
[7] F.R. Chen, G. Coudurier, J.F. Joly and J.C. Vedrine, J. Catal. 143 (1993) 616.
[8] C.X. Guo, S. Yao, J.H. Cao and Z.H. Qian, Appl. Catal. A 107 (1994) 229.
[9] D.A. Ward and E.I. Ko, J. Catal. 150 (1994) 18.
[10] T. Lei, W.M. Hua, Y. Tang, Y.H. Yue and Z. Gao, Chem. J. Chin. Univ. 21 (2000) 1240.
[11] W.M. Hua, Y.H. Yue and Z. Gao, J. Mol. Catal. A 170 (2001) 195.
[12] C.L. Chen, S. Cheng, H.P. Lin, S.T. Wong and C.Y. Mou, Appl. Catal. A 215 (2001) 21.
[13] Q.H. Xia, K. Hidajat and S. Kawi, J. Catal. 205 (2002) 318.
[14] Y.Y. Sun, L. Zhu, H.J. Lu, R.W. Wang, S. Lin, D.Z. Jiang and F.S. Xiao, Appl. Catal. A 237 (2002) 21.
[15] M.V. Landau, L. Titelman, L. Vradman and P. Wilson, Chem. Commun. (2003) 594.
[16] M.A. Ecormier, A.F. Lee and K. Wilson, Micropor. Mesopor. Mater. 80 (2005) 301.
[17] Y.Y. Huang, T.J. McCarthy and W.M.H. Sachtler, Appl. Catal. A 148 (1996) 135.
[18] U. Ciesla, S. Schacht, G.D. Stucky, K.K. Unger and F. Schuth, Angew. Chem. Int. Ed. Engl. 35 (1996) 541.
[19] X. Yang, F.C. Jentoft, R.E. Jentoft, F. Girgsdies and T. Ressler, Catal. Lett. 81 (2002) 25.
[20] Y.Y. Sun, L.N. Yuan, W. Wang, C.L. Chen and F.S. Xiao, Catal. Lett. 87 (2003) 57.
[21] Z. Gao, Y.D. Xia, W.M. Hua and C.X. Miao, Top. Catal. 6 (1998) 101.
[22] Y.D. Xia, W.M. Hua, Y. Tang, Z. Gao Chem. Commun. (1999) 1899.
[23] W.M. Hua, Y.D. Xia, Y.H. Yue and Z. Gao, J. Catal. 196 (2000) 104.
[24] J.A. Moreno and G. Poncelet, J. Catal. 203 (2001) 453.
[25] P. Canton, R. Olindo, F. Pinna, G. Strukul, P. Riello, M. Meneghetti, G. Cerrato, C. Morterra and A. Benedetti, Chem. Mater. 13 (2001) 1634.
[26] W.M. Hua and J. Sommer, Appl. Catal. A 227 (2002) 279.
[27] Y.Y. Sun, L.N. Yuan, S.Q. Ma, Y. Han, L. Zhao, W. Wang, C.L. Chen and F.S. Xiao, Appl. Catal. A 268 (2004) 17.
[28] J.H. Wang and C.Y. Mou, Appl. Catal. A 286 (2005) 128.
[29] Y.Y. Sun, S. Walspurger, B. Louis and J. Sommer, Appl. Catal. A 292 (2005) 200.
[30] Z.R. Zhang and T.J. Pinnavaia, J. Am. Chem. Soc. 124 (2002) 12294.
[31] B.H. Davis, R.A. Keogh and R. Sarinivasan, Catal. Today 20 (1994) 219.
[32] R.A. Comelli, C.R. Vera and J.M. Parera, J. Catal. 151 (1995) 96.
[33] C.X. Miao, W.M. Hua, J.M. Chen and Z. Gao, Catal. Lett. 39 (1996) 406.
[34] D. Farcasiu, J.Q. Li and S. Cameron, Appl. Catal. A 151 (1997) 173.
[35] D.A. Ward and E.I. Ko, J. Catal. 157 (1995) 321.
[36] C. Morterra, G. Cerrato, F. Pinna and M. Signoretto, J. Catal. 157 (1995) 109.
[37] W. Stichert, F. Schüth, S. Kuba and H. Knözinger, J. Catal. 198 (2001) 277.

[38] C.S. John, N.C.M. Alma and G.R. Hays, Appl. Catal. 6 (1983) 341.
[39] G.D. Yadav and A.D. Murkute, Adv. Synth. Catal. 346 (2004) 389.
[40] V.M. Benitez, J.C. Yori, C.R. Vera, C.L. Pieck, J.M. Grau and J.M. Parera, Ind. Eng. Chem. Res. 44 (2005) 1716.
[41] Z. Gao, J.M. Chen, W.M. Hua and Y. Tang, Stud. Surf. Sci. Catal. 90 (1994) 507.
[42] H. Matsuhashi, M. Tanaka, H. Nakamura and K. Arata, Appl. Catal. A 208 (2001) 1.
[43] B.J. Xu, W.M. Hua, Y.H. Yue, Y. Tang and Z. Gao, Catal. Lett. 100 (2005) 95.